



**HAL**  
open science

## **Design and Control of the Humanoid Robot COMAN+: Hardware Capabilities and Software Implementations**

Francesco Ruscelli, Luca Rossini, Enrico Mingo Hoffman, Lorenzo Baccelliere,  
Arturo Laurenzi, Luca Muratore, Davide Antonucci, Stefano Cordasco, Nikos  
G. Tsagarakis

► **To cite this version:**

Francesco Ruscelli, Luca Rossini, Enrico Mingo Hoffman, Lorenzo Baccelliere, Arturo Laurenzi, et al..  
Design and Control of the Humanoid Robot COMAN+: Hardware Capabilities and Software Implementations. IEEE Robotics and Automation Magazine, 2024, pp.2-13. 10.1109/MRA.2024.3505773 .  
hal-04876463

**HAL Id: hal-04876463**

**<https://hal.science/hal-04876463v1>**

Submitted on 9 Jan 2025

**HAL** is a multi-disciplinary open access archive for the deposit and dissemination of scientific research documents, whether they are published or not. The documents may come from teaching and research institutions in France or abroad, or from public or private research centers.

L'archive ouverte pluridisciplinaire **HAL**, est destinée au dépôt et à la diffusion de documents scientifiques de niveau recherche, publiés ou non, émanant des établissements d'enseignement et de recherche français ou étrangers, des laboratoires publics ou privés.

# Design and Control of the Humanoid Robot COMAN+

Francesco Ruscelli<sup>†</sup>, Luca Rossini<sup>†</sup>, Enrico Mingo Hoffman<sup>\*†</sup>, Lorenzo Baccelliere<sup>†</sup>, Arturo Laurenzi<sup>†</sup>, Luca Muratore<sup>†</sup>, Davide Antonucci<sup>†</sup>, Stefano Cordasco<sup>†</sup>, and Nikos G. Tsagarakis<sup>†</sup>

**Abstract**—Despite the prevalence of robots operating within controlled environments such as industries, recent advancements in both autonomy and human-robot interaction have expanded the potential for their use within a diverse range of scenarios. Research efforts in humanoid robotics aim to develop platforms possessing the requisite versatility and dexterity to mimic human motion. This allows such machines to perform complex tasks alongside humans while ensuring safety during operations. Following these principles, this paper presents the robot COMAN+, focusing on its hardware capabilities and software implementations. COMAN+ is developed by the Humanoid and Human Centred Mechatronics Research Line at Istituto Italiano di Tecnologia: a human-sized torque-controlled humanoid assembled with a focus on robustness, reliability, and strength. Its custom-made actuation system and sturdy yet lightweight skeleton make it ideal for working in rough conditions with a high power-to-weight ratio for heavy-duty tasks.

**Index Terms**—Humanoid robot designs; Control; Sim-to-real gap; Loco-manipulation, Safety.

## I. INTRODUCTION

A huge progression in autonomy and performance, combined with the progress in human-robot interaction, brought robots outside of industrial environments: this transition was marked by robots becoming more and more capable of working in more unstructured and diverse scenarios. These platforms are proving to be a useful resource to replace manpower in repetitive and strenuous tasks, access hazardous locations, and, more recently, operate in urban or domestic scenarios side-to-side with the general public rather than trained workers.

In robotics, there are different degrees of specialization of the platform: while most robots are built explicitly for one or a few tasks (i.e., assembling, transportation, inspection, etc.), the category of bio-inspired robots, which is becoming more and more popular, find their strength in versatility. The choice of flexibility, in terms of the range of capabilities that a single robot possesses, is increasing, even in industrial scenarios, due to the advancements in articulated locomotion and versatile interaction with the environment, i.e., the ability to navigate and interact with any surroundings. The humanoid form is the

<sup>†</sup> Humanoid and Human Centered Mechatronics (HHCM) Lab, Istituto Italiano di Tecnologia (IIT), Via Morego 30, 16163 Genova, Italy. E-mail: {francesco.ruscelli, luca.rossini, lorenzo.baccelliere, arturo.laurenzi, luca.muratore, davide.antonucci, stefano.cordasco, nikos.tsagarakis}@iit.it

<sup>\*</sup> Inria Nancy Grand Est, 615 rue du Jardin Botanique, 54600 Villers les Nancy, France. E-mail: enrico.mingo-hoffman@inria.fr

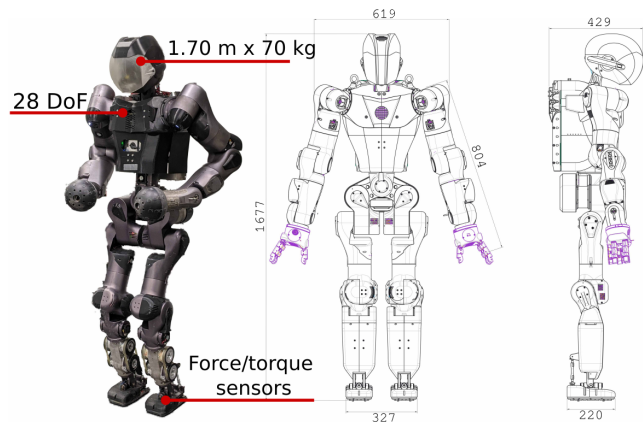


Fig. 1. Outline of the humanoid robot COMAN+.

most favorable among many bio-inspired robotic platforms, given that artificial environments are primarily designed and tailored to the human form.

With these premises, the Humanoid and Human Centered Mechatronics (HHCM) lab at Istituto Italiano di Tecnologia (IIT) developed COMAN+, third generation bipedal robot of the line after COMAN [1] and WALK-MAN [2]. The name COMAN+ refers to the second iteration of COMAN, which stands for COMpliant huMANnoid. Unlike the predecessors, COMAN+ was designed with a size and weight falling within the ranges of an adult person, as depicted in Figure 1.

The robot design aims to endow the system with resilience and power: physical capabilities ideal for carrying out tasks in unstructured, rough environments with heavy loads and powerful interactions. This is achieved by incorporating critical performance characteristics, such as custom-built high torque and power density actuators, compact torque sensors on each motor for full torque control, and a resilient frame for harsh physical interactions. These properties indicate its potential for operation with strength and reliability in harsh environments. The structure elasticity given by the Series Elastic Actuators [3](SEA) architecture allows shock absorption and a degree of compliance and protection with the surroundings. Finally, a critical prerequisite is safety.

One important milestone that pointed the research community towards the development of humanoids was the DARPA Robotics Challenge (DRC) started in 2013 and concluded in 2015, a bench-marking event where humanoid robots had to execute complex tasks for disaster response, supervised by humans. Following this event, new humanoid robots were

TABLE I  
COMPARISON OF COMAN+ WITH OTHER HUMANOID ROBOTS.

	COMAN+	HRP-5P	TALOS	JAXON	TOCABI	E2-DR
Height [mm]	1677	1820	1750	1880	1800	1680
Weight [kg]	70	101	95	127	100	85
Total DoFs	28	37	32	35	33	33
Head	0	2	2	2	2	1
Arm	2 × 8	2 × 7	2 × 7	2 × 8	2 × 7	2 × 8
Hand	2 × 1	2 × 2	2 × 1	2 × 1	2 × 1	2 × 1
Waist	2	3	2	3	2	2
Legs	2 × 6	2 × 6	2 × 6	2 × 6	2 × 6	2 × 6

built, displaying different physical structures and abilities. It is worth mentioning some recent full-size humanoids that fall in a similar category as COMAN+ for their hardware design and torque-controlled motors: TORO [4], TALOS [5], E2-DR [6], and TOCABI [7], up to the latest achievement from Boston Dynamics, the new ATLAS, which demonstrated how new-generation robots can outperform humans in terms of strength and dexterity.

This paper provides a complete overview of the robotic platform COMAN+, both in terms of construction and operation: the mechanical characteristics are described in Chapter II, while the software infrastructure and control strategies are presented in Chapter III. Finally, Chapter IV provides an overview of the projects in which COMAN+ was involved, highlighting the practical applications and the relative control scheme formulated.

## II. MECHANICAL OVERVIEW

As the third generation humanoid robot developed at the HHCM, COMAN+ inherits numerous traits from its predecessors COMAN and WALK-MAN, while introducing several improvements to its performance. The robot's body structure is human weight and size compatible, with a weight of 70 kg, a height of 1.70 m, and a width between the shoulders of 0.6 m. The arm length deviates from anthropomorphic ratios with a span-to-height ratio of roughly 1.2, intentionally designed to increase the robot's manipulation workspace in cluttered scenarios. COMAN+ was designed based on three leading criteria:

- passive compliance, through series elastic actuation;
- physical sturdiness, through resilient custom-made actuation systems and mechanical structure;
- high power density, through strong torque output from compact actuators.

Figure 1 depicts the robotic platform and its dimensions. The development of COMAN+ involves the design and fabrication of all mechanical and electrical components of the robot and the assembling of the actuation with the designed robot's structure.

### A. Actuation

The actuation system of COMAN+ is fully developed at IIT. Each actuator on the robot's joint comprises custom brushless DC motors connected to a harmonic drive gearbox, along with a fixed elastic element positioned between the

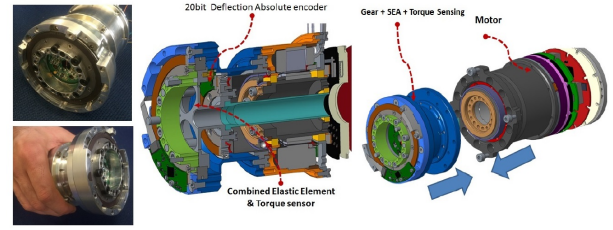


Fig. 2. The design principle of the COMAN+ actuation.

gearbox output and the load, see Figure 2. The specification of COMAN+'s actuators are listed in Table II in terms of power, torque, velocity, dimension and weight. More details about the actuators are presented in [8]. This design principle follows the SEA scheme: while decreasing the bandwidth of the motor, it comes with many advantages useful for a robot designed to work in unstructured environments and alongside humans: it decouples the high geared-inertia of the motor from the actuation link side, provides passive, intrinsic adaptation to disturbances, and it enhances the tolerance to impact loads. The torsional bar deflection at each motor is monitored by strain gauges, which improves torque sensing and enables high-fidelity torque control. The motor design is optimized for dimensions and weight without reducing the nominal and peak torque requirements for a full-sized humanoid. The semi-flexible body structure resulting from incorporating SEA actuators in the robot draws upon the intrinsic elasticity of human muscles. These actuators provide physical protection to the transmission against high bandwidth impacts, while their mechanical compliance makes them adaptable to the environment and facilitates moderate disturbance rejection. In particular, the series elastic elements protect the gearing reduction unit (i.e., harmonic drive) against impacts, enhancing the physical sturdiness of the overall system. In short, these high-performance modules deliver high torque capacity while being compliant and robust, making them well-suited for physical interaction and heavy manipulation tasks. Similar to its predecessor WALK-MAN, COMAN+ has 28 degrees of freedom (DoFs): 7 joints for each arm, 6 for each leg, and 2 for the torso. A comparison of the robot specification with other humanoid robots is shown in Table I. The motors at each joint are available in five different sizes, listed in Table II, to meet weight, speed, and torque output requirements:

- red: hip roll, hip pitch, knee pitch;
- orange: shoulder pitch, shoulder roll, torso roll;
- yellow: shoulder yaw, elbow pitch, ankle pitch, ankle roll, torso yaw, hip yaw;
- dark green: forearm yaw, forearm pitch;
- light green: wrist yaw.

Each actuator features intrinsic torque-sensing capabilities, an encoder to measure absolute joint position, and a temperature sensor to monitor its state.

### B. Upper body Design

The torso of COMAN+ counts one DoF along the yaw and the roll axes, enabling motion in the transverse and frontal

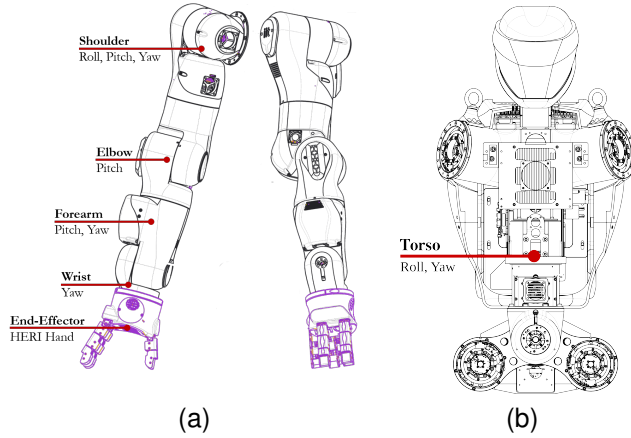


Fig. 3. Kinematic structure of COMAN+ arm (a) and torso (b).

Arm Joints Motion Range			
Joint	Motion description	Human Range (deg)	COMAN+ Range (deg)
1	Shoulder Flexion/Extension	[+180,-80]	[+210,-110]
2	Shoulder Abduction/Adduction	[+180,-50]	[+200,0]
	Shoulder Rotation	[+90,-90]	[+150,-150]
3	Elbow	[+145,0]	[+145,-20]
4	Forearm Rotation	[+90,-90]	[+150,-150]
5	Shoulder Flexion/Extension	[+90,-70]	[+90,-90]
	Wrist rotation	[+80,-80]	[+150,-150]




Fig. 4. The joint range of motion of the COMAN+ arm and a series of poses demonstrating the upper body motion range.

planes. Although removing the degree of freedom in the sagittal direction reduces the robot's range of motion for the pelvis of the robot, the first pitch joint at each leg compensates for this limitation. The arm's design follows the nominal anthropomorphic structure, providing kinematic redundancy that facilitates the setting of position and orientation of the end-effector during manipulation and interaction tasks. The shoulder joint comprises three actuators, the elbow joint features one pitch joint, and the forearm has a yaw joint for rotation. The wrist has two degrees of freedom: pitch and roll joint. Figure 3b depicts the kinematic structure of the robot's torso.

Even though this is a traditional design that aims to replicate the anthropomorphic structure of the human arm with 7-DoFs, it is only approximately equivalent to the human arm's kinematic structure. Indeed, humans can elevate (upward/downward) and incline (forward/backward) the shoulder joint, utilizing supplementary kinematic redundancy of the arm to achieve certain goals in task coordinates.

An optimization was performed to enhance the front side workspace of the upper body, evaluating important manipulation indices:

- the Product of Total and Common Workspace Area (PTCWA);
- the Global Isotropy Index (GII) for each arm within the common workspace, which measures of the end-effector isotropy;
- the Dual-arm Manipulability Index (DMI) within the common workspace.

The values of the upward angle and forward angle of COMAN+ shoulder frame were derived considering some rep-

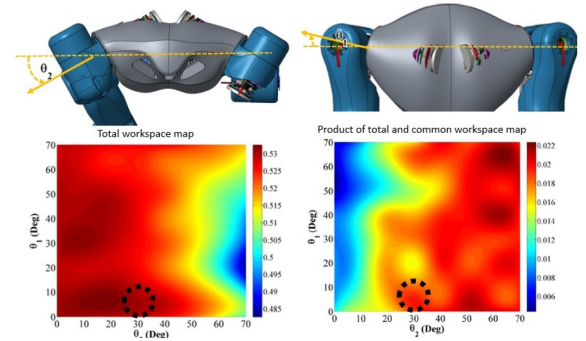


Fig. 5. The COMAN+ arm shoulder frame upward and forward angle selection.

resentative target tasks. Figure 5, depicts the total workspace map and PTCWA w.r.t the orientation of the shoulder.

The range of motion for the arm's joints was defined considering human data, data from other successful humanoid bi-manual systems, and simulation studies of a set of manipulation tasks: the range of motion of the standard human arm was used as a starting point. Wherever it was possible, a greater range of motion with respect to the human arm range was considered to enhance the motion and manipulation capability of the arm. In particular, the range of upper and lower arm rotations was extended. Similarly, the range of elbow joints was increased by considering an off-center elbow joint arrangement that results in a wider elbow flexion with respect to human elbow flexion. Finally, the wrist flexion joint range was extended to provide a larger range than that of the human wrist flexion. Results from the arm design are depicted in Figure 4, which compares the human and COMAN+ arm range of motion.

The robot's arm can manipulate over 10 kg over the entire workspace, demonstrating high power density. The wrist joint allows switching between interaction tools easily, depending on the assigned task. As for now, different end-effectors were successfully integrated and used: the anthropomorphic soft-hand [9], ideal for delicate interaction, two manipulators designed for industrial scenarios and simpler end-effectors consisting of rubber-coated ball-hands or metal plates, both of which are useful for physical interactions with the environment or heavy manipulation tasks.

### C. Lower Body Design

The lower body of the robot is developed to resemble the human structure. To improve the dynamic performance of the legs, the design aims to maximize peak velocity and acceleration, minimizing weight and inertia while ensuring that the system can withstand impacts with minimal risk of mechanical failure or malfunction. Each leg of the robot is equipped with three DoF at the hip, one DoF at the knee, and two DoFs at the ankle, as illustrated in Figure 6.

To reduce the inertia of the limbs, the leg mass is concentrated at the hip while the actuators of the ankle have been integrated into the shin. In particular, the pitch and roll actuators of the ankle of COMAN+ were positioned above the ankle, along the shin, and connected to the ankle through



TABLE II  
SPECIFICATIONS OF COMAN+ ACTUATORS.

Actuator size (colour)	Gear ratio	Maximum velocity	Torque (in Nm) peak-continuous	TS Resolution (in Nm)	Power (in W) peak-continuous	Diameter (in mm)	Length (in mm)	Mass (in kg)
Large (Red)	120	8.8rad/s	268 – 92	0.2	2096 – 778	98	166	1.73
	160	6.6rad/s	314 – 123					
Medium (Orange)	160	3.9rad/s	147 – 81	0.07	1014 – 295	93	163	1.45
Medium (Yellow)	160	6.1rad/s	147 – 46	0.07	820 – 259	93	150	1.28
Small (Dark Green)	100	11.7rad/s	55 – 17	0.07	556 – 179	82	127	1.00
Small (Light Green)	100	20.4rad/s	28 – 9	0.07	518 – 167	82	120	0.87

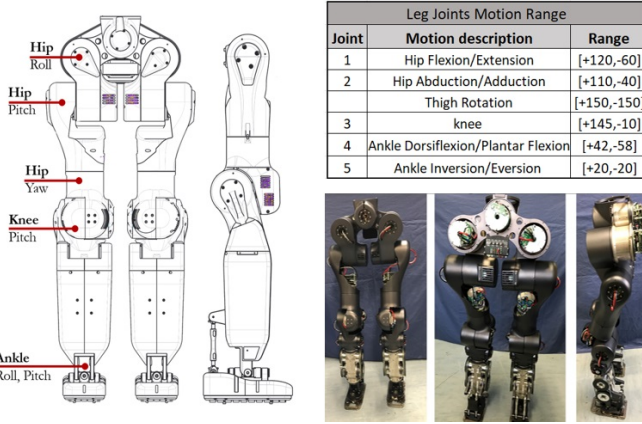


Fig. 6. Kinematic structure and assembly of the COMAN+ legs.

a dual four-bar mechanism. Thus, the weight can be shifted upwards along the tibia, moving the ankle actuation system away from the ankle and closer to the knee. The ankle mechanism is composed of a kinematic loop connecting a moving component to a fixed base, resulting in the typical configuration of the ankle with a roll and a pitch DoF.

Concentrating the leg mass as close as possible to the waist, where the robot's center of mass (CoM) is located, allows for faster swing motion and reduces coupling between lower-body and upper-body movement. It also decreases the otherwise high magnitude of shocks resulting from frequent impacts, avoiding abrupt rebounds that would destabilize the robot and increase the risk of system failures. Moreover, reducing the leg inertia also decreases energy consumption and torque requirements. Finally, compared to a serial motor arrangement for the ankle, the torque profile of the proposed ankle mechanism is preferable, as it distributes the load evenly, enabling the use of identical motors to actuate the pitch and the yaw of the ankle. However, this configuration results in a narrower range of motion, limited by the parallel mechanism limits. Furthermore, it raises the complexity of the mechanism due to the coupling between the two DoFs and the distance between the motor and the joint. The displacement of a single motor does not directly generate the motion of one DoF. Instead, achieving a pure pitch motion requires both motors operating in the same direction (common mode), whereas a pure roll requires one motor rotating opposite to the other (differential mode), as shown in Figure 7. To control the full range of motion of the ankle, a Jacobian matrix must be extracted [10] to map the motor space to the joint space, as the

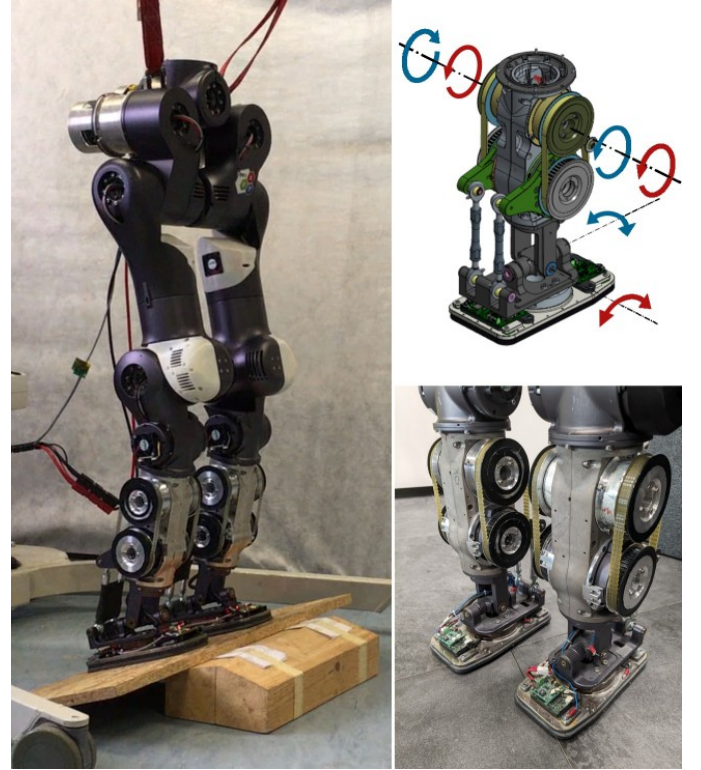


Fig. 7. The legs of the humanoid robot COMAN+. Active compliance enables the robot to adapt to terrain features like inclined surfaces. A dual four-bar mechanism connects the motors with the ankle joint. This reduces the inertia at the extremity of the leg.

joint and motor angles are related through forward kinematic mapping:

$$\begin{aligned} \dot{\mathbf{q}} &= \mathbf{J}_l(\boldsymbol{\theta}_m)\dot{\boldsymbol{\theta}}_m, \\ \boldsymbol{\tau}_m &= \mathbf{J}_l(\boldsymbol{\theta}_m)^T \boldsymbol{\tau}_j, \end{aligned} \quad (1)$$

where  $\mathbf{J}_l(\boldsymbol{\theta}_m) \in \mathbb{R}^{2 \times 2}$  is the Jacobian of the parallel ankle mechanism,  $\dot{\mathbf{q}} \in \mathbb{R}^2$  are the joint-side velocities,  $\boldsymbol{\theta}_m, \dot{\boldsymbol{\theta}}_m \in \mathbb{R}^2$  are the motor-side positions and velocities respectively,  $\boldsymbol{\tau}_m \in \mathbb{R}^2$  the motor torques, and  $\boldsymbol{\tau}_j \in \mathbb{R}^2$  the joint torques. The full derivation of the Jacobian matrix can be found in [10]. The foot plate integrates a rubber layer to absorb shock and increase grip on the ground. A six-axis force-torque sensor is attached to each foot to detect impacts, while an Inertial Measurement Unit (IMU) is installed at the pelvis level.

### III. COMAN+ SOFTWARE ARCHITECTURE

This section describes the software architecture that powers the platform COMAN+. Similarly to the hardware, the whole

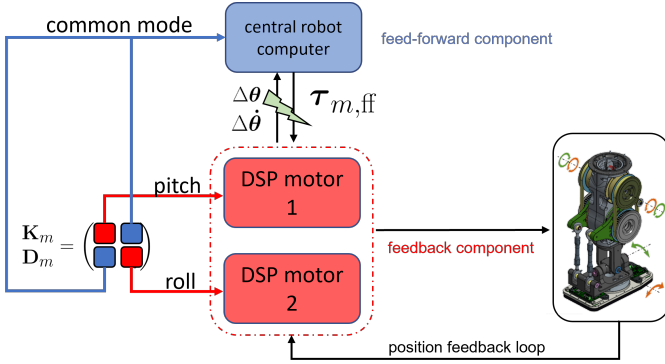


Fig. 8. Scheme of the semi-centralized impedance controller (SCIC).

software architecture is custom, from the actuators' firmware to the operator layer interface. The software modules developed for COMAN+ are designed with versatility and usability in mind to simplify the use of the robot when prototyping motion and executing high-level tasks.

The core software architecture is organized into four layers:

- the lowest level control at the actuators' level, where the decentralized controller is implemented, presented in Subsection III-A;
- a hardware manager, running in the central pc, responsible for synchronizing, sending and receiving commands to the electronic boards in each robot's actuator, presented in III-B;
- a middleware provides the communication layer between the robot (both the real hardware and the model in simulation) and the high-level commands, presented in III-C;
- an intermediate level of software units that simplify the control of the robot, presented in III-D.

The software presented in this Section is developed by the HHCM lab, using the programming languages C, C++ and Python. The last item is a set of software developed to streamline the control of COMAN+, providing modules that, over time, became the backbone of the robot control, joining the core architecture as its outer shell closer to the operator level.

#### A. Lower-level control

The decentralized joint controller at each actuator is based on an impedance control formulation that uses measured motor position, velocities, and torques. This lower-level control is implemented on a dual-core microcontroller embedded in the actuators and relies only on the measurements of the individual unit.

1) *Fail-safe Impedance Controller*: Conforming and adapting to external disturbances is essential for improving humanoid robots' interaction skills. The SEA actuators of COMAN+ guarantee a certain amount of mechanical compliance with the robot's structure. Nevertheless, robust locomotion and complex interactions require lower-level active compliance: impedance control schemes are an effective solution for robotics systems that experience frequent interactions with the

environment [11]. Due to the parallel ankle design features, a kinematic mapping exists between joint and motor velocities, as described in 1. This mapping is propagated down to the computation of the desired stiffness and damping matrices at the joint-side:

$$\{\mathbf{K}_m, \mathbf{D}_m\} = \mathcal{T}\{\mathbf{K}_j, \mathbf{D}_j\}, \quad (2)$$

where  $\mathbf{K}_m \in \mathbb{R}^{2 \times 2}$ ,  $\mathbf{D}_m \in \mathbb{R}^{2 \times 2}$  are the the motor-side matrices, and  $\mathbf{K}_j \in \mathbb{R}^{2 \times 2}$ ,  $\mathbf{D}_j \in \mathbb{R}^{2 \times 2}$  the joint-side matrices. It should be noted how a desired generic diagonal joint stiffness matrix  $\mathbf{K}_j$  is mapped into a non-diagonal motor stiffness matrix  $\mathbf{K}_m$ , resulting in a coupling between the ankle axes' pitch and roll. A detailed description to compute the desired reference joint-side stiffness matrix is found in [12]. While different versions of compliant architecture (passive or active) are used on state-of-the-art robots for human-robot interaction, not many can withstand system failures, such as communication interruptions between the central computer and the motors, that could compromise the hardware integrity or the safety of humans.

Similarly to the traditional counterpart, the semi-centralized impedance controller (SCIC) proposed in [12] allows for adaptations to the environment and partial energy absorption from impacts, mimicking the elasticity of human muscles. However, unlike fully centralized methods, this controller is immune to instabilities that can cause local joint torque controllers to lose their torque reference inputs. This results in safer robot reactions, which is particularly important for human-robot interaction and hardware protection.

While the SCIC scheme can be applied to any actuator on the robot, it was first implemented on the robot's ankles. Since the foot continuously interacts with the terrain, a degree of compliance could improve its stability on uneven grounds, as the step would conform to the surfaces and act as a filter for minor disturbances. Furthermore, given the critical role of the ankle system in standing and locomoting, ensuring a safe response would increase the full system stability in the presence of interruptions between the on-board centralized computer and actuation DSP controllers. In [12], it is demonstrated how these types of failures, i.e., interruption in the torque references of the actuators, could lead to dangerous behaviors due to unwanted torques commanded abruptly to the robot.

The SCIC leverages the joint impedance controller implemented on each DSPs, sending the desired torque as two components. The first depends only on local measurements of the actuators, i.e. the reference and the sensed position, while the second term is sent as a feed-forward torque computed by the high-level centralized controller. This decentralization allows, in the presence of failures, to hold the last motor position reference sent before the communication interruption, while the feed-forward torque is left as a bounded disturbance that is easily rejected.

The SCIC formulation (detailed in Figure 8) is defined as the following:

$$\boldsymbol{\tau}_{m,d} = \bar{\mathbf{K}}_m \Delta \boldsymbol{\theta} + \bar{\mathbf{D}}_m \Delta \dot{\boldsymbol{\theta}} + \boldsymbol{\tau}_{m,ff}, \quad (3)$$

where:

$$\boldsymbol{\tau}_{m,ff} = \tilde{\mathbf{K}}_m \Delta \boldsymbol{\theta} + \tilde{\mathbf{D}}_m \Delta \dot{\boldsymbol{\theta}} + \mathbf{J}^\top \boldsymbol{\tau}_{j,ff}. \quad (4)$$

where the matrices  $\mathbf{K}_m$  and  $\mathbf{D}_m$  are derived from the joint-motor transformation:

$$\begin{aligned} \mathbf{K}_m &= \overline{\mathbf{K}}_m + \widetilde{\mathbf{K}}_m, \\ \mathbf{D}_m &= \overline{\mathbf{D}}_m + \widetilde{\mathbf{D}}_m, \end{aligned} \quad (5)$$

where  $\overline{(\cdot)}_m$  contains the diagonal elements and  $\widetilde{(\cdot)}_m$  contains the off-diagonal elements of the matrix. Each row of the first two terms in (3) are computed in each DSP separately: the  $i^{\text{th}}$  DSP, connected to the  $i^{\text{th}}$  actuator, has enough information (position  $\theta_i$  and velocity  $\dot{\theta}_i$ ) to compute the relative torques. The remaining  $\tau_{m,\text{ff}}$  component in (4) which depends on both motors ( $\theta_i$  and  $\dot{\theta}_i$ ,  $\forall i = 1, 2$ ), is computed on the on-board computer through the off-diagonal terms  $\widetilde{\mathbf{K}}_m$  and  $\widetilde{\mathbf{D}}_m$ . The SCIC is successfully implemented on COMAN+ and experimental results validate it, both in terms of accuracy and effectiveness.

### B. Hardware manager

The decentralized low-level structure, consisting of the DSPs inside each actuator electronic board, is connected through the EtherCAT fieldbus to a central embedded PC running the Xenomai3 real-time operating system. The HHCM lab developed a custom framework, i.e. EtherCAT master, responsible for managing the network of EtherCAT slaves (i.e., the electronic boards) by exchanging suitable datagrams called Process Data Object (PDO), the real-time transmission and reception of motor references. The master implementation is a modified version of the Simple Open Ethercat Master (SOEM), as described in [8].

### C. Middleware interface

The middleware that provides a flexible interface with the robot is XBot2, detailed in [13], a custom software developed at HHCM for robotic applications. It is characterized by a modular structure that provides seamless support for multi-threaded, mixed real-time (RT), and non-RT architectures. XBot2 supplies a ready-to-use hardware abstraction layer (R-HAL) that can be modified according to the type of robot hardware to be integrated. Communication between high-level software and the robot is established by providing a specific implementation to an abstract layer containing the dynamics/kinematics model information, regardless of its specific structure. This layer connects with EtherCAT-based robots and with popular simulation environments (i.e. Gazebo, PyBullet, and MuJoCo), through a simple interface that must be compiled by the user, depending on the environment selected. XBot2 infrastructure grants a flexible Input/Output (I/O) interface that allows requesting data and sending commands to user-defined programs, i.e. plugins, running in RT loops using the well-established publish/subscribe pattern: callbacks can be defined from publishers, subscribers, or service servers. This paradigm ensures an expandable software structure: the Plugin Handler dispatches any user-defined plugin and executes it in an RT thread. Alongside the real-time thread, a companion thread allows non-real-time (NRT) programs to run, managing asynchronous communication with RT threads.

Finally, XBot2 conforms to state-of-the-art robotics standards, providing seamless interaction with ROS, the most widespread robotics middleware, and ensuring wide compatibility for component integration.

### D. Intermediate layer

The centralized control architecture takes place in the COM Express module on board of the robot or a desktop PC as a pilot PC for tethered control using a GigaBit Ethernet interface. The higher level comprises an infrastructure of software units that allows for simpler control of COMAN+ besides the direct joint-level control:

- CartesI/O [14]: a framework for the Cartesian control of hyper-redundant robots. It allows the execution of online Cartesian trajectories within a hard real-time (RT) control loop.
- CartesI/O-planning: a wrapper of CartesI/O that extends it with whole-body sampling-based planning;
- Interaction controller [15]: a module for online force control with a specific focus on floating-base robots, where under-actuation and contact forces must be considered.

### E. High-level pipeline

Two complete pipelines were developed for the robot COMAN+, leveraging the software infrastructure to endow the robot with key capabilities for a humanoid robot: the first focuses on the robot's locomotion, while the second tackles the two-fold problem of whole-body motion and environment interaction, reported in Figure 9.

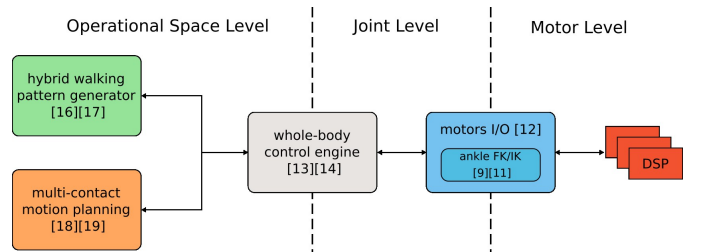


Fig. 9. Planning and control pipelines used in COMAN+. The Operational Space layer transforms user inputs, such as CoM linear velocities or goal poses, into plans that are tracked by a whole-body controller. The resulting outputs in terms of joint references are then transformed into motor commands, considering the closed parallel linkages on the ankles. Each module has the corresponding paper reference.

1) *Hybrid Walking Pattern Generator*: A novel walking pattern generator (WPG) was designed for bipedal locomotion on the robot COMAN+. The WPG combines two structurally different strategies based on the virtual constraints (VC) and the preview control to generate a stepping motion based on a few user inputs, such as duration, clearance, and stride. The inputs can be pre-planned offline or modified online to allow for side-stepping, steering, or backward stepping. The WPG draws directly from the limit cycle theory, which produces cyclic period-one gaits. An in-depth analysis of the hybrid paradigm is formulated in [16] and [17]: in the sagittal direction, it uses the VC to design a template periodic motion. Along the lateral

plane, it relies on the Preview Control, by modeling the robot as a one-dimensional linear inverted pendulum model (LIPM) that satisfies the ZMP stability criterion. Virtual Constraints (VC) simplify the complex system of humanoid robots into a lower-dimensional system, resulting in a lighter computational load than classical WPGs. The hybrid WPG generates open-loop walking of the real robot in the absence of external disturbances.

2) *Multi-Contact Motion Planning and Control Framework:* Free-floating platforms such as bipeds are highly redundant systems subject to non-linear constraints due to their inherent under-actuation that generates a strong coupling between physical interaction and body equilibrium. In addition to this, traditional limitations of classical fixed-base robots are due to kinematic reachability alongside obstacles and self-collision avoidance. The pipeline must consider multiple contacts, balancing, and collision, while the hardware platform requires accurate sensing and execution, reliability, and high power.

The pipeline for planning and control is versatile enough to generate a vast range of complex real-world physical interaction tasks that involve highly non-linear motion due to obstacles, kinematic constraints, and narrow spaces. To validate both the software and hardware capabilities of COMAN+, two tasks involving locomotion and multi-contact interaction are chosen. Being COMAN+, a high-performance robot, they can be chosen as heavy-duty and physically demanding. A complete pipeline description and its validation on the robot COMAN+ is found in [18] and [19]. The algorithm produces motions for any given physical interaction task involving quasi-static motions, even for robotic platforms characterized by poor flexibility due to their kinematic structure.

Towards physical autonomy, a second iteration of the pipeline was developed to relax the assumption of a-priori known contact location of the previous formulation. The whole-body motion planner has been coupled with a *contact space planner* that automatically selects a discrete acyclic contact sequence using a pre-defined set of end-effectors allowed to interact with the environment. Generally speaking, the set of end-effectors can also include upper-body links allowing more complex multi-contact motions not limited to the classic cyclic bipedal locomotion. Given a discrete set of contacts planned by the contact space local planner, the whole-body planner finds a continuous trajectory in joint space that moves on the manifold defined by each set of active contacts, in the so-called *foliation*.

#### IV. COMAN+ APPLICATIONS

COMAN+ was used as a testbed for many applications in different contexts. It served as a robotic platform to prove theoretical results and was used to experimentally validate complex projects, resulting in the development of reliable software modules that became valuable assets for the HHCM lab. At the same time, the platform itself was extensively tested for various motions that verified its physical performance and rough physical interaction requirements, spanning from bipedal and quadrupedal locomotion to heavy interaction with the environment. The approaches employed and the

experiment conducted on the platform are detailed in this section, demonstrating COMAN+ high strength and physical robustness<sup>1</sup>.

##### A. Locomotion

The robot can walk on flat terrains, as shown in Figure 10a, in the absence of disturbances. However, the proposed hybrid WPG is insufficient for a more robust implementation due to model inaccuracies, impacts, and floor irregularities. Integrating a compliant stabilizer [11], did not improve the robustness of walking as expected. To overcome this limitation, a more refined strategy for stabilization and disturbance rejection was attempted using an ankle and torso stabilizer. Although simulation results were promising, implementing this strategy on a real robot remains challenging due to the need for accurate sensing and control. Experimental data on this task are collected in [16] and [17].

##### B. Wall-plank

The first iteration of the multi-contact pipeline presented in III was employed on COMAN+ to execute a *wall plank*, as shown in Figure 10d, where the robot keeps the whole body suspended from the ground in a four-limbed stance where the weight is distributed between the two feet placed on a wall and the hands on the ground. This experiment shows how the software architecture can successfully bring the robot to the desired body configuration and demonstrates how the robot can exert enough torque to hold a challenging pose. The components of the pipeline that made this real-hardware application possible are the following:

- gradient-based algorithm for the computation of the contacts and the interaction forces through the centroidal dynamics under quasi-static assumption based on a post-optimization [15] before mapping them to joint torques.
- a sample-based planner using the full kinematic model to query a sequence of robot poses from a multi-contact stance to another. It guarantees feasible stances regarding joint limits, self-collisions, and singular configuration while ensuring kinematic reachability and stability.
- the generation of a feasible, time-optimal trajectory carried out by an optimization-based interpolation of the planned sequence that satisfies velocity and acceleration constraints. The experimental results of this application are shown in [18].

##### C. Multi-Contact Multi-Modal Locomotion

A demanding demo that simulates mixed gait locomotion in an obstructed scenario is devised as a further experiment to showcase the feasibility of the motions planned by the second iteration of the multi-contact planner, composed of the contact space and whole-body planner, as shown in Figure 10c: the robot is required to reach a destination that lies beyond a narrow passage from its starting point. Due to its narrow dimensions, the robot can overcome the obstacle only by

<sup>1</sup>A comprehensive collection of experiments on COMAN+ can be found at <https://zenodo.org/uploads/13788865>



passing below it, beyond which a wall can be used to stand up. The motion is particularly challenging for the robot’s geometry, which does not have a human’s full flexibility and mobility. Complex physical interaction tasks that go beyond nominal walking are still challenging for real hardware platforms: the combination of hardware and software capabilities demonstrates how COMAN+ can bridge the gap between simulation and real hardware applications, achieving robust physical mobility and dexterity. Work [19] contains all the experimental data and graphs of the multi-contact experiment.

#### D. Box picking

A manipulation experiment was set up for COMAN+ to pick and lift a box from the ground. While the motion is simpler than the demanding tasks described in the previous sections, it served as a testbed for an in-depth analysis that compared a LASSO-based Inverse Kinematics approach against a QP-based IK for whole-body applications. The controller demonstrated how the role of sparsity in the context of hyper-redundant mechanisms produces motion that favors joint motion’s parsimony instead of engaging all the available DoF, resulting in a bowing motion in which the robot keeps an ergonomic upright posture for the torso joints, while most of the movement is executed by the arms and legs to approach the object. A second experiment used the same box-picking motion for a demo that combined visual object localization, whole-body control, and real-time compliant stabilization. The main modules exploited for this project were XBotCore and CartesI/O. Figure 10b shows a sequence of frames of COMAN+ executing the box-picking task. The full paper providing an in-depth project analysis can be found in [14].

#### E. Collaborative transportation

An example of human-robot collaboration was designed to validate the framework proposed in [20]. The experiment consisted of a weight-holding and transporting task using COMAN+ alongside the human operator, as shown in Figure 10e. The main contribution of this work is a strategy to autonomously adapt the robot’s impedance in response to the amplitude of the forces exerted by the robot. When the robot moves freely, its impedance settings are low to minimize dangerous movements and collisions. On the contrary, when the robot is transporting a payload, the impedance is autonomously raised to reduce discrepancies in tracking performances that low-impedance settings can induce. This enables automatic adjustment of stiffness levels in different Cartesian directions, naturally adapting to disturbances from load variations while allowing smooth motion in less heavily loaded directions. Details of the framework and the experimental data can be found in [20].

### V. CONCLUSION

This paper presented the robot COMAN+, describing the hardware structure and the software planning and control architectures that power it. The robot was developed under

the CogIMon<sup>2</sup>. project to integrate the robot’s robust and dependable whole-body interaction capabilities and, in particular, to demonstrate heavy-duty interaction tasks in rough environments. The results of this platform, described in Chapter IV, are manifold, spanning from bipedal locomotion to heavy environment interaction involving all the limbs. The custom electronics and actuators proved to be effective in powering COMAN+, both in nominal walking and manipulation scenarios and in demanding tasks such as the wall plank and the quadrupedal locomotion. Constructing the hardware accelerated the progress of software architecture within the HHCM laboratory, as the robot was utilized as a test platform for challenging demonstrations that required the development of new software components. The robust low-level control of the robot relied on the torque sensor at the actuator level, enabling precise torque, impedance, and position control.

A prerequisite of a robot used in human-robot operations is being inherently safe: reducing the effects of failure that could compromise the hardware integrity and the safety of surrounding humans. To this end, a novel modification in the low-level control improved the reliability of the platform, allowing the robot to fail gracefully in the presence of potential system failures, i.e., communication interruption or breakdowns of the main on-board computer that, with the conventional impedance control implementation could lead to abrupt robot motions and dangerous behaviors. Regarding the higher behavioral level, the robot was used in many applications involving locomotion, manipulation, and environment interaction. It was the testbed for a novel lightweight walking pattern generator. Even without a stabilization layer, the robot executed a series of steps commanded by open-loop trajectories. COMAN+ showed excellent results in physically demanding and complex tasks, highlighting the role of multi-contact interactions in any motion beyond nominal walking. In uncontrolled and non-stationary environments, robot motion is limited to the quasi-static regime: the robot completes a challenging activity for the average human being, the wall-plank, consisting of a stance where the weight is distributed on four limbs, two feet on the wall and two hands on the ground. These motions require strength and flexibility: while COMAN+ is endowed with powerful actuators that easily support the robot throughout heavy-duty tasks, the intrinsic limitations of the humanoid platform heavily reduce the flexibility of the structure, increasing the complexity of this particularly challenging task. However, the robot still successfully executed them.

### VI. FUTURE WORK

Humanoid research seeks to obtain dexterous and autonomous robots capable of mimicking the motion skills of a human being, involving locomotion, manipulation and, more in general, interaction with the environment. Successful results were achieved both concerning the locomotion and the interaction of the biped, strategies designed and implemented on COMAN+ showed positive results. Future work will revisit

<sup>2</sup>The CogIMon project was funded by the European Union’s Horizon 2020 robotics program ICT-23-2014, under Grant Agreement 644727 (<https://cordis.europa.eu/project/id/644727>)

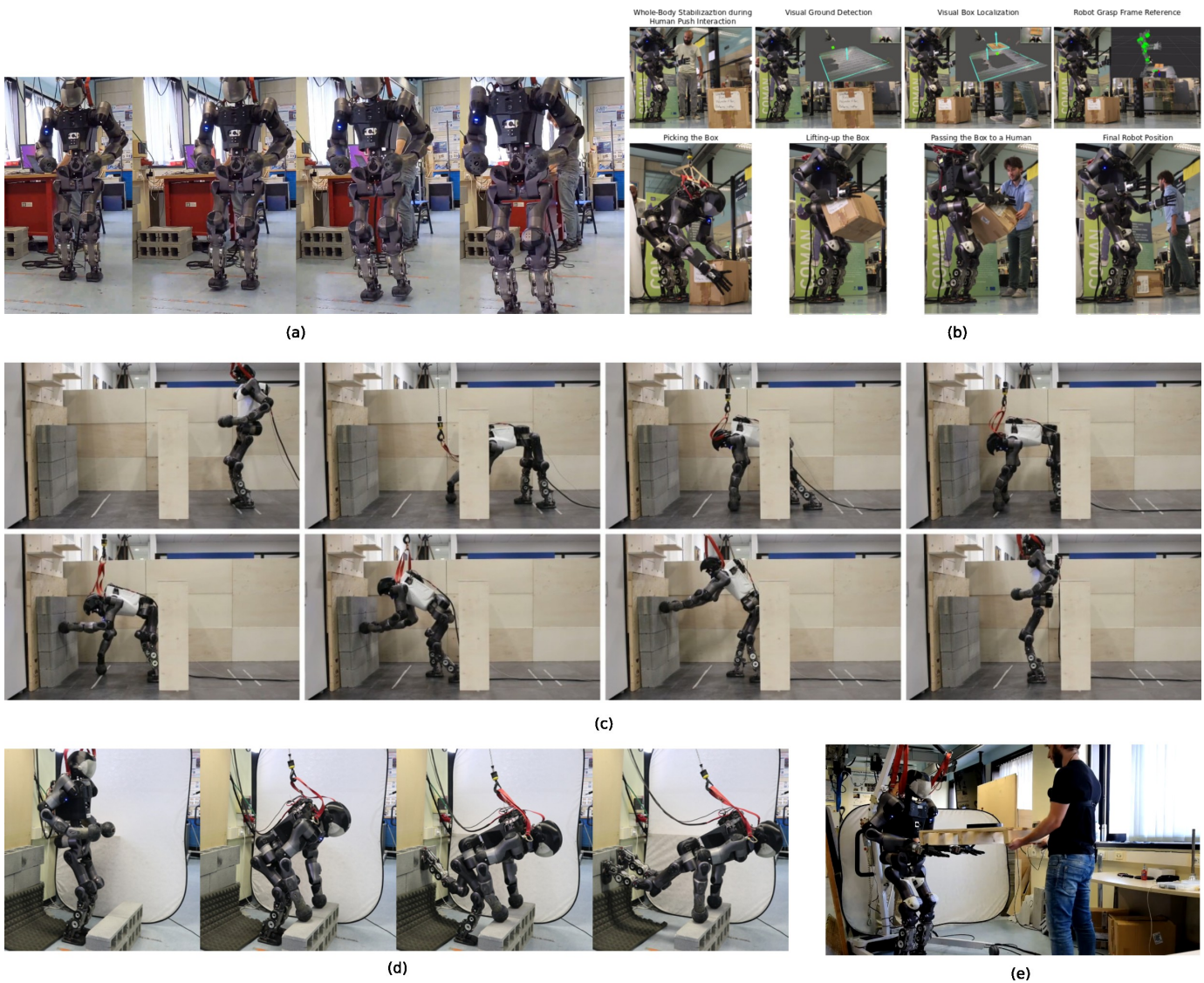


Fig. 10. COMAN+ robot applications: (a) walking using the hybrid walking pattern generator. (b) autonomous box pick-up. (c) quadrupedal walking and standing-up using the wall. (d) execution of the *wall plank* pose, in which its weight is distributed among the four limbs pushing against the wall and the bricks. (e) collaborative transportation task along with the human operator.

the design of the limbs, allowing for more dynamics and reactive motions: this would make the platform more effective for a rich repertoire of locomotion skills.

The fail-safe controlled tested on the ankles will be extended to the whole set of joints, granting active compliance and inherent safety against hardware failures. A full pipeline for robust locomotion is being developed, replacing the existing one. Closing the loop on the robot sensor and adding visual perception will increase robustness and enable the robot to overcome tasks heavily dependent on the environment conformation.

#### ACKNOWLEDGEMENTS

The research leading to these results has received funding from the European Union Horizon 2020 robotics program [ICT-23-2014], grant agreements n.644727 (CogIMon).

#### REFERENCES

- [1] N. G. Tsagarakis, S. Morfey, G. Medrano Cerda, L. Zhibin, and D. G. Caldwell, "Compliant humanoid coman: Optimal joint stiffness tuning for modal frequency control," in *2013 IEEE International Conference on Robotics and Automation*, 2013, pp. 673–678.
- [2] N. G. Tsagarakis, D. G. Caldwell, F. Negrello, W. Choi, L. Baccelliere, V. Loc, J. Noorden, L. Muratore, A. Margan, A. Cardellino, L. Natale, E. Mingo Hoffman, H. Dallali, N. Kashiri, J. Malzahn, J. Lee, P. Kryczka, D. Kanoulas, M. Garabini, M. Catalano, M. Ferrati, V. Varicchio, L. Pallottino, C. Pavan, A. Bicchi, A. Settimi, A. Rocchi, and A. Ajoudani, "WALK-MAN: A High-Performance Humanoid Platform for Realistic Environments," *Journal of Field Robotics*, vol. 34, no. 7, pp. 1225–1259, oct 2017.
- [3] G. Pratt and M. Williamson, "Series elastic actuators," in *IEEE/RSJ International Conference on Intelligent Robots and Systems (IROS)*, vol. 1, 1995, pp. 399–406.
- [4] J. Engelsberger, A. Werner, C. Ott, B. Henze, M. A. Roa, G. Garofalo, R. Burger, A. Beyer, O. Eiberger, K. Schmid, and A. Albu-Schäffer, "Overview of the torque-controlled humanoid robot toro," in *2014 IEEE-RAS International Conference on Humanoid Robots*, 2014, pp. 916–923.
- [5] O. Stasse, T. Flayols, R. Budhiraja, K. Giraud-Esclasse, J. Carpentier, J. Mirabel, A. Del Prete, P. Souères, N. Mansard, F. Lamiraux, J.-P. Laumond, L. Marchionni, H. Tome, and F. Ferro, "TALOS: A new

- humanoid research platform targeted for industrial applications,” in *International Conference on Humanoid Robotics, ICHR, Birmingham 2017*, ser. IEEE-RAS 17th International Conference on Humanoid Robotics (Humanoids), Birmingham, United Kingdom: IEEE, Nov. 2017. [Online]. Available: <https://hal.archives-ouvertes.fr/hal-01485519>
- [6] T. Yoshiike, M. Kuroda, R. Ujino, Y. Kanemoto, H. Kaneko, H. Higuchi, S. Komura, S. Iwasaki, M. Asatani, and T. Koshiishi, “The experimental humanoid robot e2-dr: A design for inspection and disaster response in industrial environments,” *IEEE Robotics & Automation Magazine*, vol. 26, no. 4, pp. 46–58, 2019.
- [7] M. Schwartz, J. Sim, J. Ahn, S. Hwang, Y. Lee, and J. Park, “Design of the humanoid robot tocabi,” in *IEEE-RAS 21st International Conference on Humanoid Robots (Humanoids)*, 2022, pp. 322–329.
- [8] N. Kashiri, L. Baccelliere, L. Muratore, A. Laurenzi, Z. Ren, E. M. Hoffman, M. Kamedula, G. F. Rigano, J. Malzahn, S. Cordasco, P. Guria, A. Margan, and N. G. Tsagarakis, “Centauro: A hybrid locomotion and high power resilient manipulation platform,” *IEEE Robotics and Automation Letters*, vol. 4, no. 2, pp. 1595–1602, 2019.
- [9] M. G. Catalano, G. Grioli, E. Farnioli, A. Serio, C. Piazza, and A. Bicchi, “Adaptive synergies for the design and control of the pisa/iit soft hand,” *The International Journal of Robotics Research*, vol. 33, no. 5, pp. 768–782, 2014.
- [10] C. Zhou and N. G. Tsagarakis, “On the comprehensive kinematics analysis of a humanoid parallel ankle mechanism,” *Journal of Mechanisms and Robotics*, 2018. [Online]. Available: <https://api.semanticscholar.org/CorpusID:125790167>
- [11] C. Zhou, Z. Li, J. Castano, H. Dallali, N. G. Tsagarakis, and D. G. Caldwell, “A passivity based compliance stabilizer for humanoid robots,” in *2014 IEEE International Conference on Robotics and Automation (ICRA)*, 2014, pp. 1487–1492.
- [12] F. Ruscelli, A. Laurenzi, E. Mingo Hoffman, and N. G. Tsagarakis, “A fail-safe semi-centralized impedance controller: Validation on a parallel kinematics ankle,” in *IEEE/RSJ International Conference on Intelligent Robots and Systems*, Madrid, Spain, Oct 2018, pp. 1–9.
- [13] A. Laurenzi, D. Antonucci, N. G. Tsagarakis, and L. Muratore, “The xbot2 real-time middleware for robotics,” *Robotics and Autonomous Systems*, vol. 163, p. 104379, 2023.
- [14] A. Laurenzi, E. Mingo Hoffman, L. Muratore, and N. G. Tsagarakis, “CartesIO: A ROS Based Real-Time Capable Cartesian Control Framework,” in *IEEE International Conference on Robotics and Automation*, 2019.
- [15] A. Laurenzi, E. Mingo Hoffman, M. Parigi Polverini, and N. G. Tsagarakis, “Balancing control through post-optimization of contact forces,” in *2018 IEEE-RAS 18th International Conference on Humanoid Robots (Humanoids)*, 2018, pp. 320–326.
- [16] F. Ruscelli, A. Laurenzi, E. M. Hoffman, and N. G. Tsagarakis, “Synchronizing virtual constraints and preview controller: a walking pattern generator for the humanoid robot coman+,” in *IEEE/RSJ International Conference on Intelligent Robots and Systems*, 2019, pp. 3876–3881.
- [17] F. Ruscelli, A. Laurenzi, E. Mingo Hoffman, and N. G. Tsagarakis, “Omnidirectional walking pattern generator combining virtual constraints and preview control for humanoid robots,” *Frontiers in Robotics and AI*, vol. 8, 2021. [Online]. Available: <https://www.frontiersin.org/articles/10.3389/frobt.2021.660004>
- [18] F. Ruscelli, M. P. Polverini, A. Laurenzi, E. M. Hoffman, and N. G. Tsagarakis, “A multi-contact motion planning and control strategy for physical interaction tasks using a humanoid robot,” in *2020 IEEE/RSJ International Conference on Intelligent Robots and Systems (IROS)*, 2020, pp. 3869–3876.
- [19] L. Rossini, P. Ferrari, F. Ruscelli, A. Laurenzi, G. Oriolo, N. G. Tsagarakis, and E. M. Hoffman, “Multi-contact planning and control for humanoid robots: Design and validation of a complete framework,” *Robotics and Autonomous Systems*, vol. 166, p. 104448, 2023.
- [20] L. Muratore, A. Laurenzi, and N. G. Tsagarakis, “A self-modulated impedance multimodal interaction framework for human-robot collaboration,” in *2019 International Conference on Robotics and Automation (ICRA)*, 2019, pp. 4998–5004.